European Journal of Medicinal Chemistry 51 (2012) 259–270

Contents lists available at SciVerse ScienceDirect

European Journal of Medicinal Chemistry

journal homepage: http://www.elsevier.com/locate/ejmech

Original article

Design of [(2-pyrimidinylthio)acetyl]benzenesulfonamides as inhibitors of human carbonic anhydrases

Edita Čapkauskaitė [a,b], Asta Zubrienė [a], Lina Baranauskienė [a], Giedrė Tamulaitienė [c], Elena Manakova [c], Visvaldas Kairys [d], Saulius Gražulis [c], Sigitas Tumkevičius [b], Daumantas Matulis [a,*]

[a] Vilnius University, Institute of Biotechnology, Department of Biothermodynamics and Drug Design, Graičiūno 8, Vilnius LT-02241, Lithuania
[b] Vilnius University, Faculty of Chemistry, Department of Organic Chemistry, Naugarduko 24, Vilnius LT-03225, Lithuania
[c] Vilnius University, Institute of Biotechnology, Department of Protein – DNA Interactions, Graičiūno 8, Vilnius LT-02241, Lithuania
[d] Vilnius University, Institute of Biotechnology, Department of Bioinformatics, Graičiūno 8, Vilnius LT-02241, Lithuania

ARTICLE INFO

Article history:
Received 14 September 2011
Received in revised form
23 February 2012
Accepted 24 February 2012
Available online 3 March 2012

Keywords:
Carbonic anhydrase isozymes
Isothermal titration calorimetry
Thermal shift assay
ThermoFluor®
Sulfonamides as CA inhibitors

ABSTRACT

A series of [(2-pyrimidinylthio)acetyl]benzenesulfonamides were designed and synthesized. Their binding affinities as inhibitors of several recombinant human carbonic anhydrase (CA) isozymes were determined by isothermal titration calorimetry (ITC) and thermal shift assay (TSA). A group of compounds containing a chlorine atom in the benzenesulfonamide ring were found to exhibit higher selectivity but lower binding affinity toward tested CAs. The crystal structures of selected compounds in complex with CA II were determined to atomic resolution. Docking studies were performed to compare the binding modes of experimentally determined crystallographic structures with computational prediction of the pyrimidine derivative binding to CA II. Several compounds bound to select CAs with single-digit nanomolar affinities and could be used as leads for inhibitor development toward a select CA isozyme.

1. Introduction

Carbonic anhydrases (CAs, EC 4.2.1.1) are ubiquitous zinc-containing metalloenzymes present in prokaryotes and eukaryotes that catalyze the reversible hydration of carbon dioxide to bicarbonate [1]. There are 15 different isozymes of human carbonic anhydrases (CA), with different tissue distributions, subcellular locations, and expression levels [2]. CAs are involved in numerous important biological processes related to respiration, pH balance, CO_2 homeostasis, electrolyte secretion in a variety of tissues/organs, gluconeogenesis, lipogenesis, ureagenesis, bone resorption, calcification, tumorigenicity, and many other physiologic or pathologic processes [2–5].

Many CA isozymes constitute valid targets for the design and development of CA inhibitors for clinical applications. There are at least 30 CA inhibitors in clinical development or clinically used drugs [2]. Diffuse localization of CA isoforms in many tissues/organs limits potential pharmacological applications [6–8]. Hence, the design of isozyme-specific inhibitors is the current challenge in the development of new therapeutic agents. Classical CA inhibitors already described are characterized by the presence of aromatic/heterocyclic sulfonamide or sulfamate/sulfamide scaffolds [7,9].

Recently, we have reported on the synthesis of benzimidazoles *N*- and *S*-alkylated with 2-chloro-5-bromoacetylbenzenesulfonamide (**I**, **II**) (Fig. 1) and the study of their CA inhibitory activity toward CA I, CA II, CA VII, and CA XIII [10]. It was found that *S*-alkylated benzimidazole derivatives bind more strongly to the tested CAs than *N*-alkylated benzimidazoles and the structurally related indapamide. Moreover, some *S*-alkylated derivatives were found to exhibit selectivity to CA II and CA VII. The study of cocrystal structures of the most active *S*-alkylated derivatives of benzimidazole with CA II revealed that the CA II-bound *S*-alkylated ligands have larger hydrogen bonding patterns due to hydrogen bonds between the *S* and *Nδ*2 atoms of Asn62 and water-mediated hydrogen bonds of the endocyclic nitrogen atoms of benzimidazole with the protein.

The study of binding details of (4-pyrimidinyl)benzenesulfonamides (**III**) with CA II showed that in the binding of sulfonamides, in which pyrimidine and benzenesulfonamide moieties are separated with a $NHCH_2CH_2$ linker, hydrophobic interactions of the ligand with the protein play the most important role [11]. We designed [(2-pyrimidinylthio)acetyl]benzenesulfonamides **1a**–**j**, **2a**–**j** (Scheme 1) in the search for more potent and selective CA inhibitors.

Abbreviations: c, cyclic form; CA, carbonic anhydrase; ITC, isothermal titration calorimetry; o, open chain form; TSA, thermal shift assay.

* Corresponding author. Tel.: +370 5 269 1884; fax: +370 5 260 2116.
E-mail addresses: matulis@ibt.lt, daumantas.matulis@bti.vu.lt (D. Matulis).

0223-5234/$ – see front matter © 2012 Elsevier Masson SAS. All rights reserved.
doi:10.1016/j.ejmech.2012.02.050

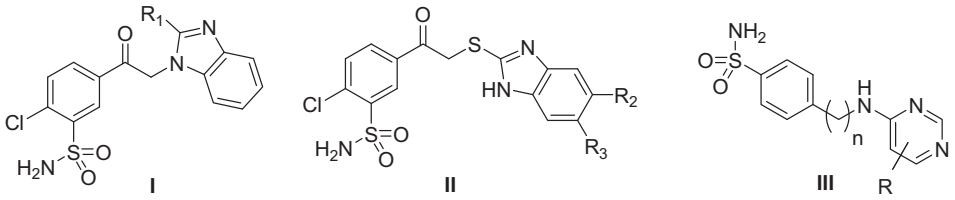

Fig. 1. Structures of *N*- and *S*-alkylated (benzimidazolyl)benzenesulfonamides **I**, **II**, and (4-pyrimidinyl)benzenesulfonamides **III**.

Furthermore, docking studies indicate that computational modeling is consistently improving in its predictive powers in compound affinities ranking and the estimation of the structural features of the protein–ligand complex. The structures of several predicted compound–protein complexes closely matched the crystallographic structures. The predictive method is increasingly useful in the design of novel CA inhibitors.

2. Results and discussion

2.1. Chemistry

S-alkylation of **a**–**j** with ω-bromoacetylbenzenesulfonamides **1** and **2** to give pyrimidine derivatives **1a**–**j** and **2a**–**j** was carried out in tetrahydrofuran at room temperature in the presence of sodium acetate (Scheme 1). For comparison, 2-chloro-5-[(phenylthio) acetyl]benzenesulfonamides **1k** and **2k** have also been synthesized by the alkylation of thiophenol (**k**) with benzenesulfonamides **1** and **2** using the same reaction conditions employed for the synthesis of **1a**–**j** and **2a**–**j**, respectively (Scheme 2).

2.2. Binding studies

The binding affinities of the [(2-pyrimidinylthio)acetyl]benzenesulfonamides (**1a**–**j** and **2a**–**j**) and [(2-phenylthio)acetyl]benzenesulfonamides (**1k** and **2k**) to recombinant human CA isozymes CA I, CA II, CA VII, and CA XIII were determined by thermal shift assay (TSA) and isothermal titration calorimetry (ITC). The observed dissociation constants for all compounds are listed in Table 1. Fig. 2 shows representative binding data obtained by TSA (isozymes CA I, CA II, and CA VII), while Fig. 3 shows representative binding data obtained by ITC (isozymes CA I and CA XIII). Both techniques were used for the measurements to obtain the most precise binding data possible. Despite good agreement between the two techniques, there were some discrepancies between the TSA and ITC data observed with CA I and, to a lesser extent, for the other three isozymes. Both the ITC and TSA experiments were repeated several times, and the discrepancies appeared to be out of the range of the standard deviations for both methods. The discrepancies appeared to be random, but the TSA data appeared to be more reliable, especially for the tightest binding cases where ITC curves were too steep to be fitted precisely.

The binding affinity of all compounds in this study ranged from approximately 4.5 μM for **1j** to approximately 1.9 nM for **2d**, both toward CA I. The ranges were smaller for other tested CAs: 9.1–200 nM (**2k** and **1a**) for CA II, 20–710 nM (**1d** and **1k**) for CA VII, and 3.5–360 nM (**2d** and **2a**) for CA XIII.

In most cases, the 2-Cl-benzenesulfonamide headgroup (compounds **1**) had lower binding affinity than benzenesulfonamide (compounds **2**). For example, **1a** bound to CA I approximately 12 times more weakly than **2a**, as shown by both TSA and ITC. The same was true for CA II, though to a lesser extent, approximately 3 times. However, CA VII bound Cl-bearing compounds **1** even stronger than compounds **2**. For example, compound **1d** bound CA VII about 9 times more strongly than **2d**.

Various aromatic rings attached to the headgroup of benzenesulfonamides have been previously tested. In a search for more selective compounds, we have synthesized a series of pyrimidine-bearing compounds. Comparison of the affinities of the pyrimidine-containing compounds (**1j** and **2j**) with compounds bearing the benzene ring (**1k** and **2k**) shows that benzene has 5–10 times stronger affinity to CA I, 1.5–2 times stronger to CA II, 1–1.3 times stronger to CA VII, and 1.3–1.5 times stronger to CA XIII. Therefore, inclusion of the pyrimidine appears to have weakened the affinity. However, pyrimidine-bearing compounds are often more selective. For example, **1j** binds CA II, CA VII, and CA XIII 6–14 times stronger than to CA I, while **1k** binds CA II, CA VII, and CA XIII only 1.3–3 times stronger than to CA I.

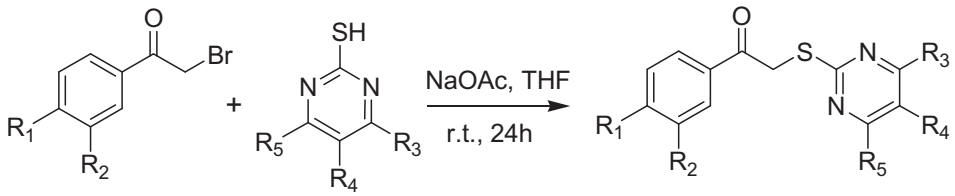

1: R_1=Cl, R_2=SO_2NH_2,
2: R_1=SO_2NH_2, R_2=H,

a-j

1a-j,
2a-j

a: R_3=OH, R_4=H, R_5=Me,
b: R_3=OH, R_4=Bn, R_5=Me,
c: R_3=OH, R_4=H, R_5=Pr,
d: R_3=OH, R_4=H, R_5=t-Bu,
e: R_3=OH, R_4=CO_2Et, R_5=H,
f: R_3=Me, R_4=H, R_5=Me,
g: R_3=H, R_4=Et, R_5=H,
h: R_3=H, R_4=Pr, R_5=H,
i: R_3=H, R_4=Bu, R_5=H,
j: R_3=H, R_4=H, R_5=H,

Scheme 1. Synthesis of compounds **1a**–**j** and **2a**–**j**.

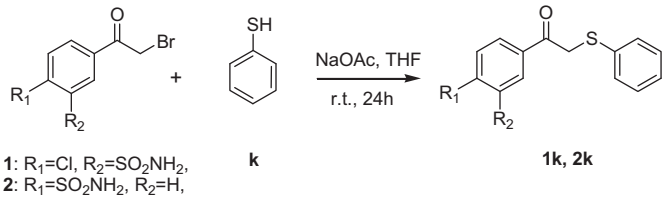

Scheme 2. Synthesis of compounds **1k** and **2k**.

The data reported in Table 1 also show that the nature of the substituent on the pyrimidine ring significantly influences the binding affinity against CA I, CA II, CA VII, and CA XIII isoforms. For example, the addition of the third ring (compounds **1a** and **2a** versus **1b** and **2b**, respectively) did not appreciably benefit the binding to CA I, CA II, and CA VII but increased the binding to CA XIII by about 5–30 times. Comparing the series of compounds bearing aliphatic tails on the pyrimidine ring (ethyl **g**, propyl **h**, and butyl **i**) shows that the tail length did not affect the binding affinity by 2 times to any of the tested CAs.

It should be noted that the dissociation constants listed in Table 1 were only observed at particular conditions, such as pH 7.0. These dissociation constants were not corrected for the linked protonation effects occurring upon ligand binding to CA. To determine an intrinsic binding constant, it is important to measure ligand association with CA at a series of pH values and in at least two buffers. Because the goal was to compare the observed dissociation constants occurring at physiological conditions, no such measurements were performed.

2.3. Crystallography

The structures of compound-CA II complex were solved to atomic resolution for compounds **1f**, **1g**, **2a**, **2f**, **2i**, and **2j**. The six compounds that were selected for soaking to CA II crystals could be divided into two groups, compounds containing Cl in the benzenesulfonamide ring (**1f** and **1g**) and compounds that do not have Cl in the ring (**2a**, **2f**, **2i**, and **2j**). The electron density maps of several compounds bound to CA II are shown in Fig. 4. The presence of chlorine determines the position of the first ring. The 2-chlorobenzenesulfonamide rings coincide perfectly in both crystal structures (Fig. 5). The benzenesulfonamide ring position in the crystal structures with inhibitors that do not contain Cl also overlap well (Fig. 6), but the planes of the first rings in both cases differ by an angle of approximately 30° (Fig. 7). Pyrimidine rings of ligands that do not contain Cl are nearly co-planar to each other.

The orientation of the first ring is defined by the tight binding of the sulfonamide group to the Zn in the active center of the protein. The Cl is trapped between hydrophobic residues Leu198, Leu141, Val143, Val121, and Val207. This binding pattern is very similar to that observed in 3M67, 3M96 and 3MYQ, as described in [10].

The conformation of the linker connecting 2-chlorobenzenesu lfonamide in **1f** and **1g** is fixed in both crystal structures by hydrogen bonds of oxygen with Gln92 and Asn67 side chains. Sulfur participates in a hydrogen bond with the amino group of Asn62. There are DMSO molecules trapped between the pyrimidine moiety of **1f** or **1g** and the protein, which was carried over from the solution of inhibitors used for soaking CA II crystals.

The position of the pyrimidine ring in both compounds was very similar. These parts of the molecules were found in the same plane as the benzimidazole in the 3M67 and 3M96 structures. This moiety is in a van der Waals contact with protein side chains that form a substrate-binding cavity.

Although ligands **2a**, **2i**, **2f** and **2j** did not contain Cl in the benzenesulfonamide ring, the ring was in a very similar position in all four structures. This position is probably defined by hydrophobic contacts with protein side chains. Leu198 supports the benzene ring, while Thr200 and Val121 restrain its mobility from both sides. The linker is positioned in such a way that carbonyl is too far away to make hydrogen bonds with polar amino acids of the substrate-binding cavity of CA II. The interaction of this group of ligands observed in crystals is mainly hydrophobic. The cyclic form **II** of compound **2f** was not found in the crystal structure.

The pyrimidine ring of inhibitor **2a** showed alternative conformations in the crystal structure. The linker in **2a** was forked after the carbonyl group, and two alternative conformations were modeled to explain the observed electron density. The pyrimidine rings in both variants overlapped, and two alternate positions for the sulfur atom of the linker were found in this structure. The electron density of the pyrimidine of **2i** was rather poor, which means that this ring was not fixed in the crystal structure, although the main conformation seems to be the modeled one.

Table 1
Synthetic compound dissociation constants to four human recombinant CA isoforms as determined by TSA and confirmed by ITC (given in brackets), both determined at 37 °C, pH 7.0.

Compound	Dissociation constants K_d (μM) to CA isoforms			
	CA I	CA II	CA VII	CA XIII
1a	0.83 (2.5)	0.20 (0.13)	0.13 (0.32)	0.20 (0.10)
2a	0.067 (0.18)	0.070 (0.050)	0.17 (0.63)	0.36 (0.71)
1b	0.45 (0.69)	0.033 (0.050)	0.14 (0.57)	0.042 (0.17)
2b	0.033 (0.10)	0.025 (0.093)	0.14 (0.38)	0.013 (0.071)
1c	0.67 (0.75)	0.067 (0.079)	0.056 (0.074)	0.056 (0.081)
2c	0.017 (0.087)	0.083 (0.061)	0.25 (0.14)	0.063 (0.068)
1d	0.10 (0.24)	0.05 (0.10)	0.020 (0.092)	0.025 (0.062)
2d	0.0019 (0.020)	0.029 (0.027)	0.18 (0.34)	0.0035 (0.037)
1e	1.2 (0.42)	0.050 (0.037)	0.025 (0.14)	0.13 (0.13)
2e	0.017 (0.10)	0.018 (0.030)	0.20 (0.10)	0.29 (0.32)
1f	1.0 (0.85)	0.22 (0.15)	0.33 (0.46)	0.33 (0.98)
2f	0.022 (0.10)	0.033 (0.052)	0.13 (0.26)	0.083 (0.13)
1g	1.8 (0.88)	0.14 (0.27)	0.33 (0.43)	0.11 (0.11)
2g	0.030 (0.11)	0.013 (0.057)	0.056 (0.12)	0.029 (0.080)
1h	1.0 (1.9)	0.10 (0.20)	0.50 (0.48)	0.067 (0.82)
2h	0.033 (0.20)	0.013 (0.037)	0.067 (0.080)	0.023 (0.020)
1i	1.4 (0.56)	0.067 (0.18)	0.20 (0.36)	0.067 (0.16)
2i	0.042 (0.27)	0.014 (0.026)	0.10 (0.20)	0.029 (0.019)
1j	4.5 (0.99)	0.33 (0.43)	0.71 (0.66)	0.33 (0.46)
2j	0.067 (0.11)	0.017 (0.012)	0.067 (0.083)	0.12 (0.077)
1k	0.83 (0.64)	0.25 (0.11)	0.71 (0.31)	0.25 (0.26)
2k	0.0067 (0.10)	0.0091 (0.077)	0.050 (0.14)	0.067 (0.28)

Average standard deviations for both methods were below 25%.

2.4. Docking studies

Compound docking simulations to CA II were performed to validate and improve computational procedures for the prediction of compound binding efficiency and structural arrangement. The docking simulations were performed using Vdock software [12].

Initially, ligands **1f** and **2j** were docked into corresponding CA II X-ray structures to verify if the experimental binding mode can be reproduced. Because of the sulfonamide nitrogen coordination with zinc in the CA binding site, the docking was expedited by fixing the sulfonamide nitrogen at the X-ray position. This was accomplished in Vdock by setting the relevant nitrogen atom as the translational center and placing it inside a zero-sized ($0 \times 0 \times 0$) translational box. This procedure removed translational degrees of freedom from the docking task and ensured the correct binding mode of the sulfonamide group. As a result, the benzenesulfonamide fragment docked very similarly to the X-ray structure.

However, the flexible, partly hydrophilic “tail” of the ligand was mostly incorrectly binding to the hydrophilic parts on the CA surface, but not to the hydrophobic pocket lined by the residues Phe131,

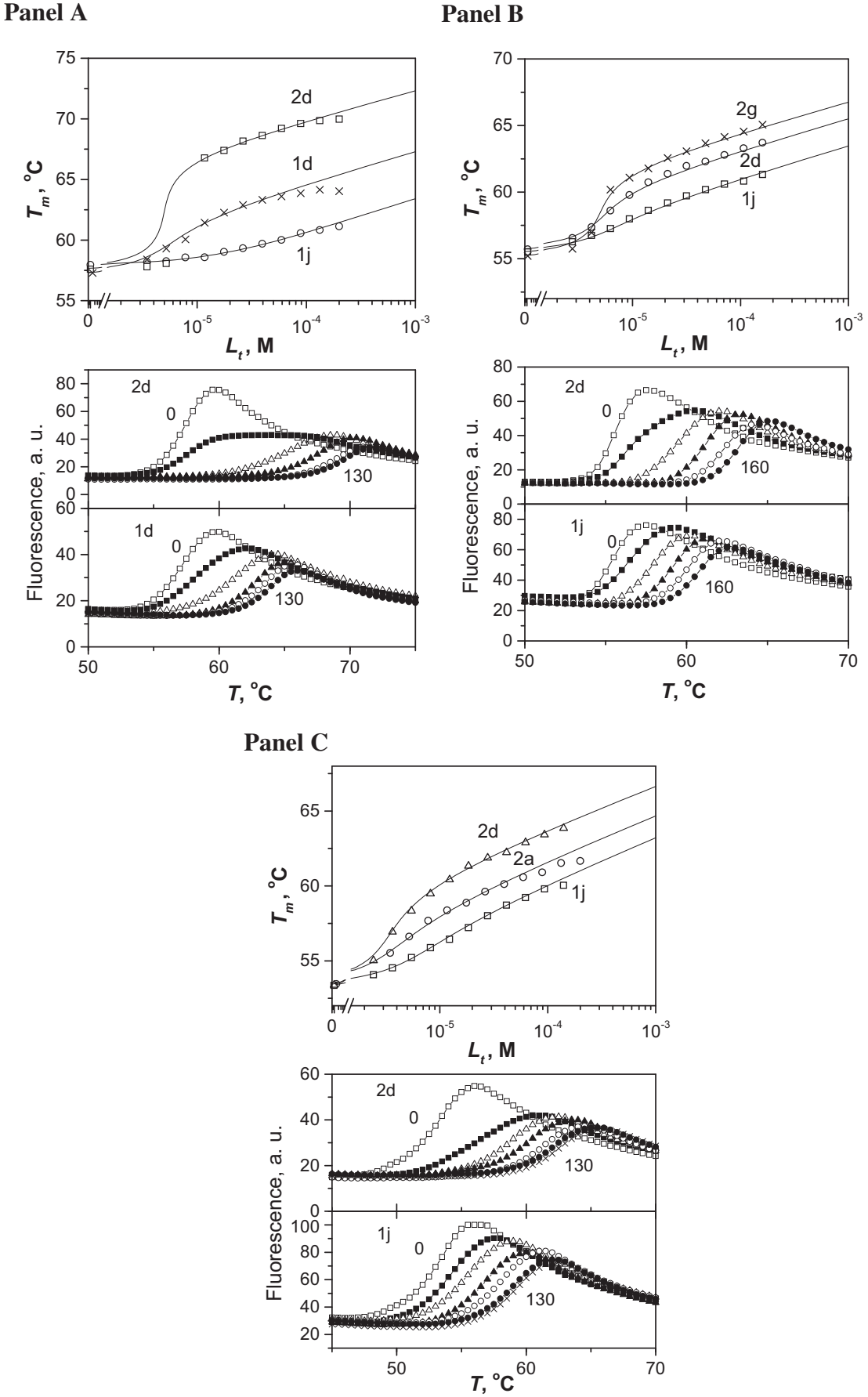

Fig. 2. TSA data of selected compound binding to CA I (Panel A), CA II (Panel B), and CA VII (Panel C). Panels on the bottom compare denaturation curves observed by fluorescence at 0 to 130 or 160 μM added ligand concentrations. Panels on the top show the dependence of the protein melting temperatures T_m on ligand concentrations.

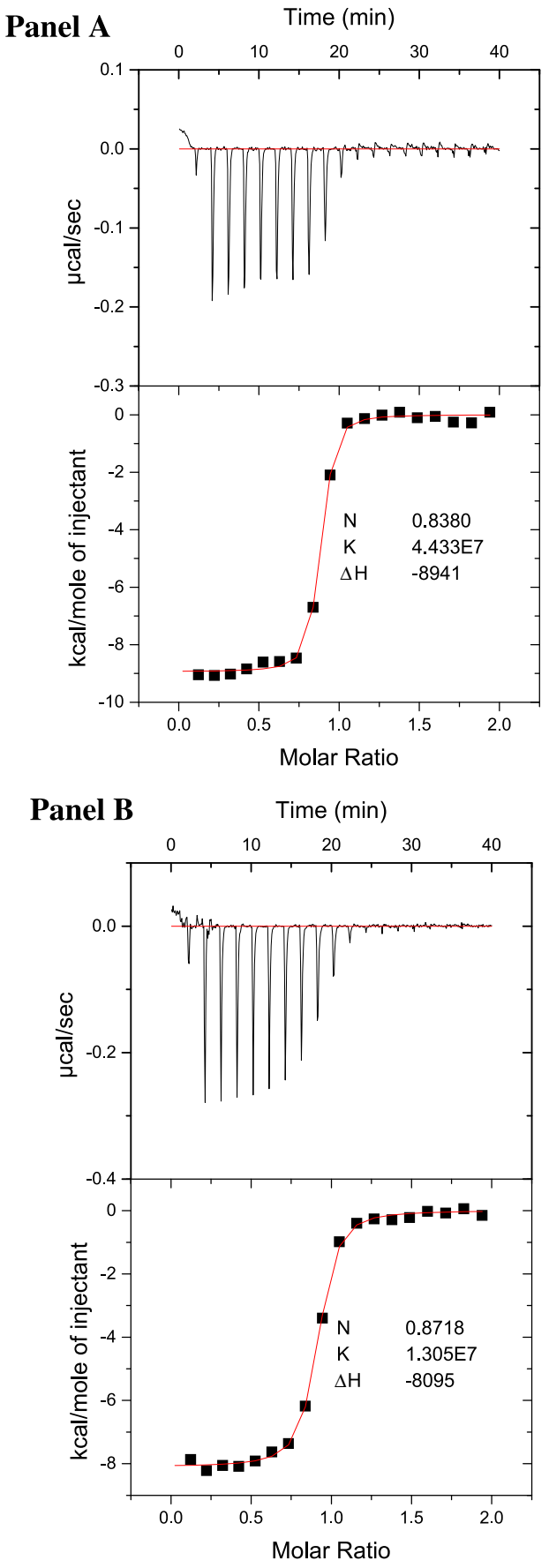

Fig. 3. ITC data of **2d** binding to CA I (Panel A) and **2j** binding to CA XIII (Panel B).

Val135, Leu198, and Pro202. Vdock allows for constraining the selected dihedrals of the ligand. We constrained five rotatable dihedrals of the ligands, starting from the sulfonamide NH_2 to the *S* of the thioether. The constrained dihedrals were allowed a ±15° variation from the original X-ray values. By using these constraints, the X-ray binding modes of docked **1f** and **2j** were reproduced with heavy atom distance root-mean-square deviation (RMSD) equal to 0.28 and 0.96 Å, respectively (Fig. 8, **1f** and **2j**). Compounds **1g**, **2a**, **2f** and **2i** were also docked into CA II, with the resulting geometries fairly close to the solved X-ray structures, with 0.56 (**1g**), 0.45 (conformation B of **2a**), 0.26 (**2f**), and 1.79 (**2i**) Å RMSD (Fig. 8). Fig. 9 shows compounds **1a**–**i** and **2a**–**i** docked using the described constraints into the CA II from the complexes with **1f** and **2j**, respectively.

The inhibitors docked closely into the hydrophobic groove on the CA surface in the X-ray structures. This geometry can be used as a basis for further application of more advanced energy-scoring functions. Fig. 10 illustrates the reasonably good correlations obtained between the experimentally observed binding energies and the calculated apparent binding affinities obtained using the Poisson–Boltzmann surface area (PBSA) approach [13]. Interestingly, the correlations were better for chlorine-containing series **1a**–**i** than the **2a**–**i** series. The outcome is likely due to **1a**–**i** sticking out into the solution more than **2a**–**i**; hence, the solvent exposed surface area approximation as a part of a continuum solvation model could be more accurate in the case of the former.

An interesting question is why the chlorine-containing compounds bind generally more poorly than the compounds without Cl in the first ring. Scott and co-workers found that the scaffold constituent of 2-Cl-benzenesulfonamide has a lesser CA II binding affinity compared to benzenesulfonamide [14]. Apparently, the chlorine-containing ligand tails reach less deeply into the hydrophobic pocket of CA II than the compounds without the chloride. This also explains the greatest difference between the affinities of the two scaffold types for ligands **1k** and **2k**: the most hydrophobic tail (benzene) of molecule **2k** (very similarly to **2j**, Fig. 9) makes good contacts within the hydrophobic pocket, while **1k**, similar to **1f**, barely reaches the groove entrance between residues Phe131 and Pro202.

These docking and PBSA results merit use in future studies, including use with different isoforms, to design isoform-specific inhibitors.

3. Conclusions

A series of aromatic sulfonamide inhibitors were designed with nanomolar affinities toward CA isozymes I, II, VII, and XIII. X-ray crystallographic cocrystal structures and computational docking studies provided structural details of inhibitor binding to CA II and demonstrated a correlation between the experimental and computed structures. Some inhibitors exhibited up to 50-times selectivity toward one or another CA isozyme. Application of two biophysical methods to measure compound binding affinities (TSA and ITC) provided a possible binding evaluation that was as accurate as possible and enabled energetics-structure correlations, with the goal of designing novel compounds with desired properties.

4. Experimental protocols

4.1. Syntheses

Synthesis of 5-(2-bromoacetyl)-2-chlorobenzensulfonamide (**1**) and 4-(bromoacetyl)benzenesulfonamide (**2**) was accomplished from commercially available 1-(4-chloro-3-nitrophenyl)ethanone and 1-(4-aminophenyl)ethanone, respectively, as described in [15] and [16]. 2-Mercaptopyrimidines **a**, **e**, **f**, **h**, and **j** are commercially

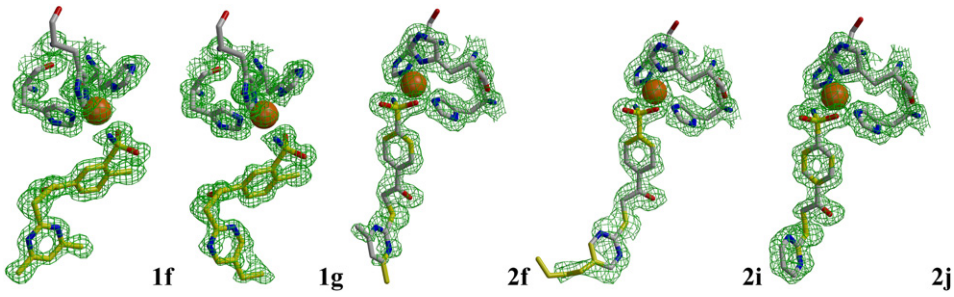

Fig. 4. View of compounds **1f**, **1g**, **2f**, **2j**, and **2i** in the active center of CA II. Zn^{2+} coordinated by His94, His96 and His119 is shown as an orange sphere. The electron density map $|2F_{obs} - F_{calc}|$ is contoured at 0.8σ. The picture was generated using MOLSCRIPT [37], Raster3D [38] and BOBSCRIPT [39]. (For interpretation of the references to colour in this figure legend, the reader is referred to the web version of this article.)

available. 6-alkyl-2-thioxo-2,3-dihydro-4(1*H*)-pyrimidinones **b** [17], **c** [18], and **d** [18] were synthesized by condensation of an appropriately substituted β-keto ester with thiourea. 5-alkyl-2(1*H*)-pyrimidinethiones **g** and **i** were prepared from thiourea and 2-alkyl-1,1,3,3-tetraethoxypropane as described previously [19]. All ingredients were purchased from Sigma–Aldrich and Alfa Aesar GmbH.

The melting points of the compounds were determined in open capillaries on a Thermo Scientific 9100 Series apparatus without further correction. IR spectra were obtained on a Perkin–Elmer FT-IR spectrophotometer Spectrum BX II in KBr. ^{1}H and ^{13}C NMR spectra were recorded on a Varian Unity Inova spectrometer (300 and 75 MHz, respectively) in DMSO-d_6 using residual DMSO signals (2.52 ppm and 40.21 ppm for ^{1}H and ^{13}C NMR spectra, respectively) as the internal standard. TLC was performed with silica gel 60 F254 aluminum plates (Merck) and visualized with UV light. High-resolution mass spectra (HRMS) were recorded on a Dual-ESI Q-TOF 6520 mass spectrometer (Agilent Technologies). The purities of target compounds were analyzed using an HPLC system with UV detection.

*4.1.1. General procedure for the syntheses of **1a**–**k** and **2a**–**k***

A mixture of the corresponding pyrimidine (**a**–**j**) or thiophenol **k** (0.539 mmol), appropriate compound **1** or **2** (0.539 mmol), and sodium acetate (49.5 mg, 0.604 mmol) in tetrahydrofuran (3 ml) was stirred at room temperature for 24 h. The reaction mixture was poured into water. The precipitate was filtered off and then washed with water and then with diethyl ether to yield **1a**–**k** or **2a**–**k**.

*4.1.1.1. 2-Chloro-5-{[(4-methyl-6-oxo-1,6-dihydropyrimidin-2-yl)thio] acetyl}benzenesulfonamide (**1a**).* Yield 78%, mp 211–213 °C. IR ν cm^{-1}: 3344, 3220 (NH_2, NH), 1698 (CO), 1634 (CONH). ^{1}H NMR δ ppm: (1:0.32) 1.94 (3H, s, CH_3, open chain form (o)), 2.18 (0.96H, s, CH_3, cyclic form (c)), 3.58 (0.32H, d, J = 12.9 Hz, $\underline{CH_2}$COH, c), 3.66 (0.32H, d, J = 12.3 Hz, $\underline{CH_2}$COH, c), 4.74 (2H, s, CH_2CO, o), 5.94 (0.32H, s, $C_{5'}$–H, c), 5.99 (1H, br s, $C_{5'}$–H, o), 7.63 (0.64H, s, $C_{3,4}$–H, c), 7.69 (0.64H, s, NH_2, c), 7.85 (2H, s, NH_2, o), 7.88 (1H, d, J = 8.7 Hz, C_3–H, o), 8.09 (0.32H, s, C_6–H, c), 8.31 (1H, dd, J = 1.8 Hz, J = 8.1 Hz, C_4–H, o), 8.53 (1H, d, J = 1.5 Hz, C_6–H, o), 10.73 (1H, br s, NH, o). HRMS calcd. for $C_{13}H_{12}ClN_3O_4S_2$ ($[M + H]^+$): 374.0031, found: 374.0032.

*4.1.1.2. (4-{[(4-Methyl-6-oxo-1,6-dihydro-2-pyrimidinyl)sulfanyl]acetyl}benzenesulfonamide) (**2a**).* Yield 75%, mp 183–185 °C. IR ν cm^{-1}: 3439, 3329, 3199 (NH_2, NH), 1699 (CO), 1649 (CONH). ^{1}H NMR δ ppm: (1:0.31) 1.96 (3H, s, CH_3, o), 2.18 (0.93H, s, CH_3, c), 3.56 (0.31H, d, J = 12.3 Hz, $\underline{CH_2}$COH, c), 3.63 (0.31H, d, J = 12.3 Hz, $\underline{CH_2}$COH, c), 4.76 (2H, s, CH_2CO, o), 5.94 (0.31H, s, $C_{5'}$–H, c), 5.98 (1H, br s, $C_{5'}$–H, o), 7.40 (0.62H, s, NH_2, c), 7.59–7.63 (2.62H, m, NH_2, o, $C_{2,6}$–H, c), 7.83

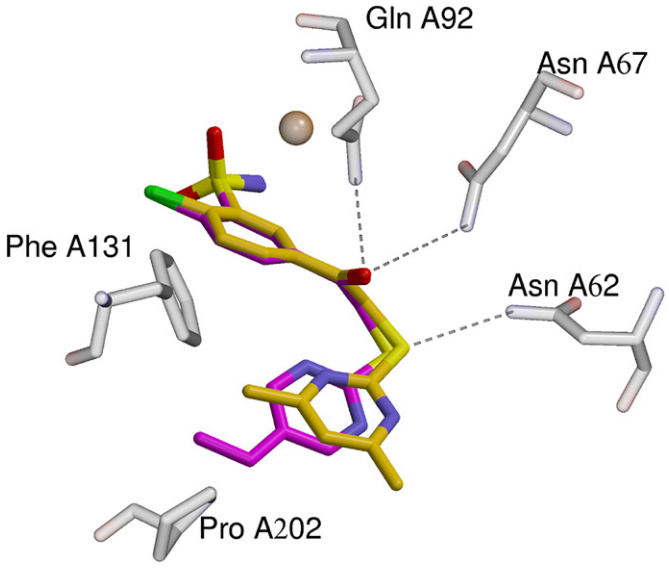

Fig. 5. View of **1f** (gold) and **1g** (magenta) located in the active center of CA II. Zn^{2+} is shown as an orange transparent sphere. The picture was generated using MOLSCRIPT [37] and Raster3D [38]. (For interpretation of the references to colour in this figure legend, the reader is referred to the web version of this article.)

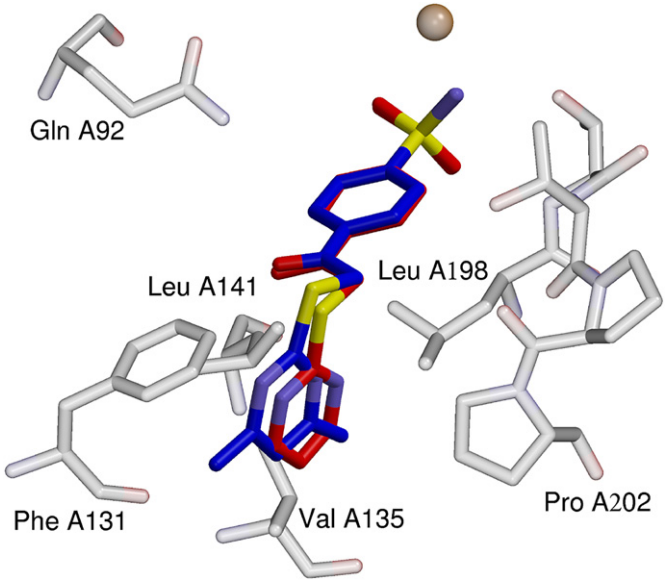

Fig. 6. View of **2f** (blue) and **2j** (red) located in the active center of CA II. Zn^{2+} is shown as an orange transparent sphere. The picture was generated using MOLSCRIPT [37] and Raster3D [38]. (For interpretation of the references to colour in this figure legend, the reader is referred to the web version of this article.)

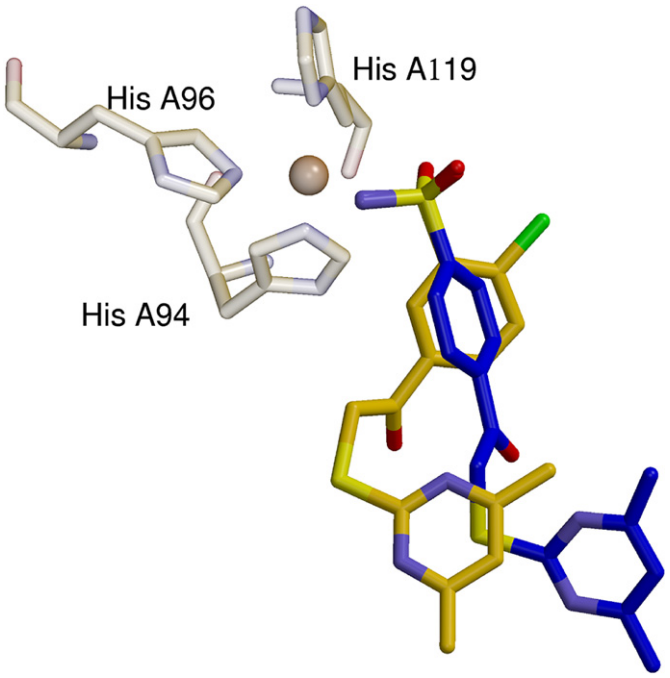

Fig. 7. View of **1f** (gold) and **2f** (blue) located in the active center of CA II. Zn^{2+} coordinated by His94, His96 and His119 is shown as an orange transparent sphere. The picture was generated using MOLSCRIPT [37] and Raster3D [38]. (For interpretation of the references to colour in this figure legend, the reader is referred to the web version of this article.)

(0.62H, d, J = 8.7 Hz, $C_{3,5}$–H, c), 8.00 (2H, d, J = 8.4 Hz, $C_{2,6}$–H), 8.22 (2H, d, J = 8.4 Hz, $C_{3,5}$–H), 12.53 (1H, br s, NH, o). HRMS calcd. for $C_{13}H_{13}N_3O_4S_2$ ([M + H]$^+$): 340.0420, found: 340.0418.

*4.1.1.3. 5-{[(5-Benzyl-4-methyl-6-oxo-1,6-dihydropyrimidin-2-yl) thio]acetyl}-2-chlorobenzenesulfonamide (**1b**).* Yield 81%, mp

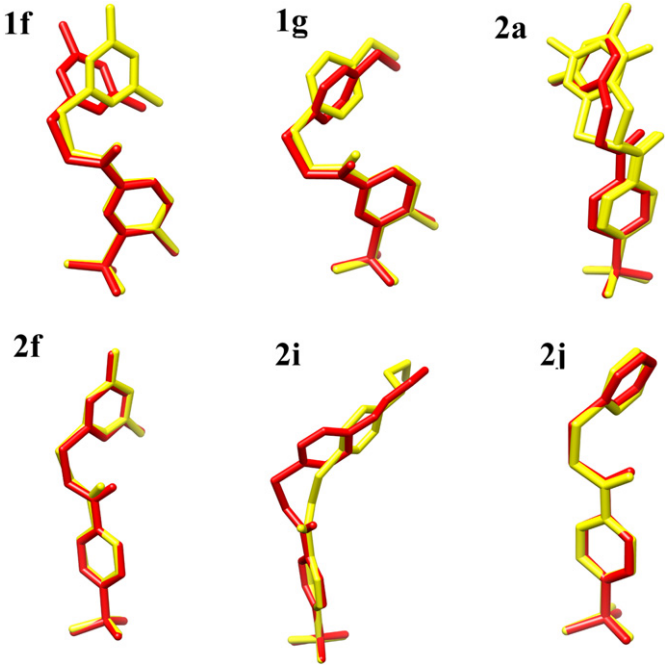

Fig. 8. Docked ligand poses (red) superposed on the X-ray structures (yellow). The constrained docking protocol was used (see text). (For interpretation of the references to colour in this figure legend, the reader is referred to the web version of this article.)

193–195 °C. IR ν cm^{-1}: 3341, 3223 (NH_2, NH), 1693 (CO), 1636 (CONH). ^{1}H NMR δ ppm: (1:0.31) 1.92 (3H, s, CH_3, o), 2.20 (0.93H, s, CH_3, c), 3.57–3.70 (3.24H, m, $\underline{CH_2}$COH, c, CH_2Ph, o, c), 4.73 (2H, s, CH_2CO, o), 7.14–7.27 (6.55H, m, Ph–H, o, c), 7.64 (0.62H, s, $C_{3,4}$–H, c), 7.69 (0.62H, s, NH_2, c), 7.86 (2H, s, NH_2, o), 7.87 (1H, d, J = 8.7 Hz, C_3–H, o), 8.16 (0.31H, s, C_6–H, c), 8.31 (1H, dd, J = 1.8 Hz, J = 8.4 Hz, C_4–H, o), 8.54 (1H, d, J = 1.5 Hz, C_6–H, o), 12.68 (1H, br s, NH, o). HRMS calcd. for $C_{20}H_{18}ClN_3O_4S_2$ ([M + H]$^+$): 464.0500, found: 464.0493.

*4.1.1.4. 4-{[(5-Benzyl-4-methyl-6-oxo-1,6-dihydro-2-pyrimidinyl)sulfanyl]acetyl}benzenesulfonamide (**2b**).* Yield 86%, mp 181–183 °C. IR ν cm^{-1}: 3315, 3243 (NH_2, NH), 1700 (CO), 1638 (CONH). ^{1}H NMR δ ppm: (1:0.32) 1.93 (3H, s, CH_3, o), 2.21 (0.96H, s, CH_3, c), 3.59 (0.32H, d, J = 12.0 Hz, $\underline{CH_2}$COH, c), 3.65 (0.32H, d, J = 12.0 Hz, $\underline{CH_2}$COH, c), 3.70 (2.64H, s, CH_2Ph, o, c), 4.76 (2H, s, CH_2CO, o), 7.15–7.28 (6.60H, m, Ph–H, o, c), 7.44 (0.64H, s, NH_2, c), 7.61–7.65 (2.64H, m, NH_2, o, $C_{2,6}$–H, c), 7.84 (0.64H, d, J = 8.1 Hz, $C_{3,5}$–H, c), 7.80 (2H, d, J = 7.5 Hz, $C_{2,6}$–H), 8.23 (2H, d, J = 8.1 Hz, $C_{3,5}$–H), 12.84 (1H, br s, NH, o). HRMS calcd. for $C_{20}H_{19}N_3O_4S_2$ ([M + H]$^+$): 430.0890, found: 430.0895.

*4.1.1.5. 2-Chloro-5-{[(6-oxo-4-propyl-1,6-dihydropyrimidin-2-yl)thio] acetyl}benzenesulfonamide (**1c**).* Yield 78%, mp 202–204 °C. IR ν cm^{-1}: 3329, 3184 (NH_2, NH), 1702 (CO), 1637 (CONH). ^{1}H NMR δ ppm: (1:0.31) 0.66 (3H, t, J = 6.8 Hz, CH_3, o), 0.92 (0.93H, t, J = 6.8 Hz, CH_3, c), 1.18–1.29 (2H, m, CH_2, o), 1.57–1.68 (0.62H, m, CH_2, c), 2.11 (2H, t, J = 6.6 Hz, CH_2, o), 2.40 (0.62H, t, J = 7.5 Hz, CH_2, c), 3.59 (0.31H, d, J = 12.6 Hz, $\underline{CH_2}$COH, c), 3.66 (0.31H, d, J = 12.6 Hz, $\underline{CH_2}$COH, c), 4.72 (2H, s, CH_2CO, o), 5.93 (1.31H, br s, $C_{5'}$–H, o, c), 7.63 (0.62H, s, $C_{3,4}$–H, c), 7.69 (0.62H, s, NH_2, c), 7.84 (2H, s, NH_2, o), 7.88 (1H, d, J = 8.4 Hz, C_3–H, o), 8.10 (0.31H, s, C_6–H, c), 8.33 (1H, d, J = 8.4 Hz, C_4–H, o), 8.53 (1H, s, C_6–H, o), 12.60 (1H, br s, NH, o). HRMS calcd. for $C_{15}H_{16}ClN_3O_4S_2$ ([M + H]$^+$): 402.0344, found: 402.0342.

*4.1.1.6. 4-{[(6-Oxo-4-propyl-1,6-dihydro-2-pyrimidinyl)sulfanyl]acetyl}benzenesulfonamide (**2c**).* Yield 78%, mp 168–170 °C. IR ν cm^{-1}: 3360, 3269 (NH_2, NH), 1699 (CO), 1657 (CONH). ^{1}H NMR δ ppm: (1:0.32) 0.66 (3H, t, J = 7.2 Hz, CH_3, o), 0.92 (0.96H, t, J = 7.2 Hz, CH_3, c), 1.27 (2H, sextet, J = 6.9 Hz, CH_2, o), 1.57–1.69 (0.64H, m, CH_2, c), 2.13 (2H, t, J = 7.2 Hz, CH_2, o), 2.41 (0.64H, t, J = 7.2 Hz, CH_2, c), 3.57 (0.32H, d, J = 12.6 Hz, $\underline{CH_2}$COH, c), 3.64 (0.32H, d, J = 12.3 Hz, $\underline{CH_2}$COH, c), 4.75 (2H, s, CH_2CO, o), 5.91–5.93 (1.32H, m, $C_{5'}$–H, o, c), 7.42 (0.64H, s, NH_2, c), 7.61 (2.64H, s, NH_2, o, $C_{2,6}$–H, c), 7.83 (0.64H, d, J = 8.4 Hz, $C_{3,5}$–H, c), 8.00 (2H, d, J = 8.4 Hz, $C_{2,6}$–H), 8.24 (2H, d, J = 8.4 Hz, $C_{3,5}$–H), 12.58 (1H, br s, NH, o). HRMS calcd. for $C_{15}H_{17}N_3O_4S_2$ ([M + H]$^+$): 368.0733, found: 368.0733.

*4.1.1.7. 5-{[(4-tert-Butyl-6-oxo-1,6-dihydropyrimidin-2-yl)thio]acetyl}-2-chlorobenzenesulfonamide (**1d**).* Yield 86%, mp 201–203 °C. IR ν cm^{-1}: 3333, 3181 (NH_2, NH), 1699 (CO), 1643 (CONH). ^{1}H NMR δ ppm: (1:0.32) 0.97 (9H, s, $(CH_3)_3$, o), 1.21 (2.79H, s, $(CH_3)_3$, c), 3.57 (0.31H, d, J = 12.6 Hz, $\underline{CH_2}$COH, c), 3.68 (0.31H, d, J = 12.3 Hz, $\underline{CH_2}$COH, c), 4.82 (2H, s, CH_2CO, o), 5.92 (0.31H, s, $C_{5'}$–H, c), 5.98 (1H, br s, $C_{5'}$–H, o), 7.63 (0.62H, s, $C_{3,4}$–H, c), 7.69 (0.62H, s, NH_2, c), 7.84 (2H, s, NH_2, o), 7.89 (1H, d, J = 8.1 Hz, C_3–H, o), 8.11 (0.31H, s, C_6–H, c), 8.34 (1H, d, J = 8.4 Hz, C_4–H, o), 8.53 (1H, s, C_6–H, o), 12.64 (1H, br s, NH, o). HRMS calcd. for $C_{16}H_{18}ClN_3O_4S_2$ ([M + H]$^+$): 416.0500, found: 416.0495.

*4.1.1.8. 4-{[(4-tert-Butyl-6-oxo-1,6-dihydro-2-pyrimidinyl)sulfanyl] acetyl}benzenesulfonamide (**2d**).* Yield 85%, mp 175–177 °C. IR ν cm^{-1}: 3303, 3178 (NH_2, NH), 1707 (CO), 1636 (CONH). ^{1}H NMR δ ppm: (1:0.25) 0.96 (9H, s, $(CH_3)_3$, o), 1.22 (2.25H, s, $(CH_3)_3$, c), 3.59 (0.25H, d, J = 12.9 Hz, $\underline{CH_2}$COH, c), 3.66 (0.25H, d, J = 12.0 Hz, $\underline{CH_2}$COH, c), 4.83 (2H, s, CH_2CO, o), 5.92 (0.25H, s, $C_{5'}$–H, c), 5.97 (1H,

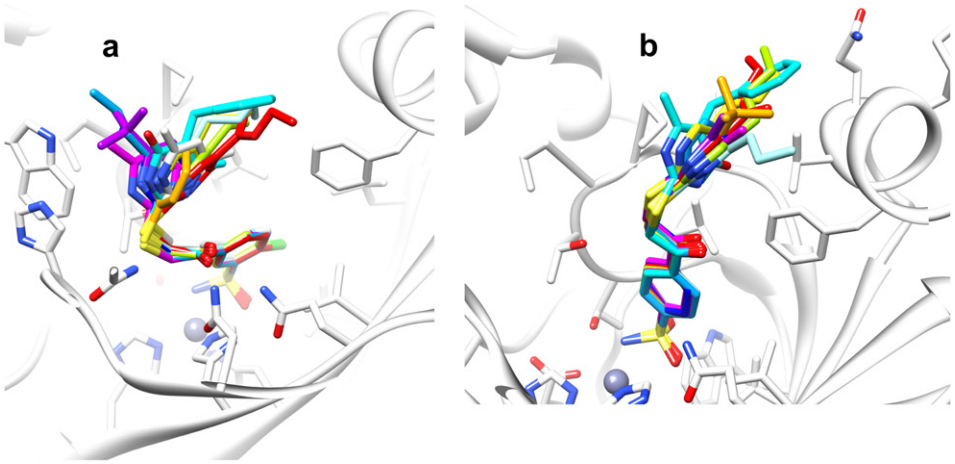

Fig. 9. Superposed compounds **1a**–**i** (a) and **2a**–**i** (b) docked to CA II (white ribbons/sticks). Docking was performed into the receptors taken from the complexes with **1f** (a) and **2j** (b) using dihedral and translational constraints (see text). The tails of the ligands extend more into the binding site in the case of non-chlorinated compounds (b).

br s, $C_{5'}$–H, o), 7.42 (0.50H, s, NH_2, c), 7.62 (2.50H, s, NH_2, o, $C_{2,6}$–H, c), 7.83 (0.50H, d, J = 8.4 Hz, $C_{3,5}$–H, c), 8.00 (2H, d, J = 8.4 Hz, $C_{2,6}$–H), 8.26 (2H, d, J = 8.4 Hz, $C_{3,5}$–H), 12.65 (1H, br s, NH, o). HRMS calcd. for $C_{16}H_{19}N_3O_4S_2$ ($[M + H]^+$): 382.0890, found: 382.0886.

*4.1.1.9. Ethyl 2-({2-[3-(aminosulfonyl)-4-chlorophenyl]-2-oxoethyl} thio)-6-oxo-1,6-dihydropyrimidine-5-carboxylate (**1e**).* Yield 87%, mp 191–193 °C. IR ν cm^{-1}: 3306 (NH_2), 1727 (COOAc), 1700 (CO), 1694 (CONH). ^{1}H NMR δ ppm: (1:0.28) 1.19–1.26 (3.84H, m, CH_3, o, c), 3.64 (0.28H, d, J = 12.9 Hz, $\underline{CH_2}$COH, c), 3.76 (0.28H, d, J = 12.6 Hz, $\underline{CH_2}$COH, c), 4.16–4.22 (2.56H, m, CH_2, o, c), 4.92 (2H, s, CH_2CO, o), 7.64 (0.28H, d, C_3–H, c), 7.70–7.74 (0.84H, m, NH_2, c, C_4–H, c), 7.85 (2H, s, NH_2, o), 7.88 (1H, d, J = 8.4 Hz, C_3–H, o), 8.17 (0.28H, d, J = 1.8 Hz, C_6–H, c), 8.28–8.31 (2H, m, $C_{4'}$–H, o, C_4–H, o), 8.45 (0.28H, s, $C_{4'}$–H, c), 8.53 (1H, d, J = 1.5 Hz, C_6–H, o), 13.44 (1H, br s, NH, o). HRMS calcd. for $C_{15}H_{14}ClN_3O_6S_2$ ($[M + H]^+$): 432.0085, found: 432.0084.

*4.1.1.10. Ethyl 2-({2-[4-(aminosulfonyl)phenyl]-2-oxoethyl}sulfanyl)-6-oxo-1,6-dihydropyrimidine-5-carboxylate (**2e**).* Yield 81%, mp 180–182 °C. IR ν cm^{-1}: 3312, 3223 (NH_2, NH), 1726 (COOAc), 1709(CO), 1684 (CONH). ^{1}H NMR δ ppm: (1:0.28) 1.19–1.27 (3.84H, m, CH_3, o, c), 3.65 (0.28H, d, J = 12.6 Hz, $\underline{CH_2}$COH, c), 3.73 (0.28H, d, J = 12.6 Hz, $\underline{CH_2}$COH, c), 4.16–4.23 (2.56H, m, CH_2, o, c), 4.94 (2H, s, CH_2CO, o), 7.43 (0.56H, s, NH_2, c), 7.62 (2H, s, NH_2, o), 7.70 (0.56H, d, J = 8.4 Hz, $C_{2,6}$–H, c), 7.85 (0.56H, d, J = 8.1 Hz, $C_{3,5}$–H, c), 8.01 (2H, d, J = 8.1 Hz, $C_{2,6}$–H), 8.23 (2H, d, J = 8.4 Hz, $C_{3,5}$–H), 8.32 (1H, s, $C_{4'}$–H, o), 8.47 (0.28H, s, $C_{4'}$–H, c), 13.45 (1H, br s, NH, o). HRMS calcd. for $C_{15}H_{15}N_3O_6S_2$ ($[M + H]^+$): 398.0475, found: 398.0470.

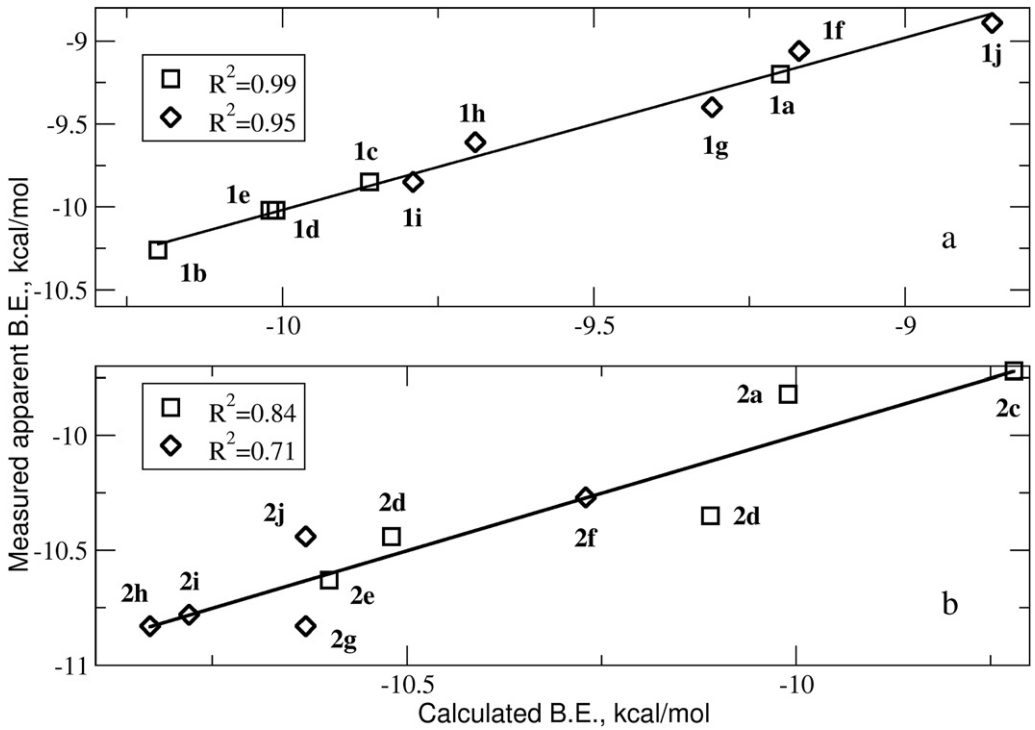

Fig. 10. Correlation between the calculated by PBSA and experimental CA II binding energies (B. E.) for the hydroxy-pyrimidine (squares) and pyrimidine (diamonds) subseries for compounds **1a**–**i** (a) and **2a**–**i** (b).

*4.1.1.11. 2-Chloro-5-{[(4,6-dimethyl-2-pyrimidinyl)sulfanyl]acetyl}benzenesulfonamide (**1f**).* Yield 93%, mp 187–189 °C. IR ν cm^{-1}: 3268 (NH_2), 1702 (CO). ^{1}H NMR δ ppm: 2.23 (6H, s, $2CH_3$), 4.70 (2H, s, CH_2CO), 6.94 (1H, s, $C_{5'}$–H), 7.84 (2H, s, NH_2), 7.88 (1H, d, J = 8.4 Hz, C_3–H), 8.33 (1H, dd, J = 2.1 Hz, J = 8.1 Hz, C_4–H), 8.54 (1H, d, J = 2.1 Hz, C_6–H). ^{13}C NMR δ ppm: 23.86 (2C), 38.03, 116.80, 128.92, 132.84, 133.55, 135.79, 136.12, 142.19, 167.74 (2C), 169.30, 194.05. HRMS calcd. for $C_{14}H_{14}ClN_3O_3S_2$ ($[M + H]^+$): 372.0238, found: 372.0238.

*4.1.1.12. 4-{[(4,6-Dimethyl-2-pyrimidinyl)sulfanyl]acetyl}benzenesulfonamide (**2f**).* Yield 78%, mp 174–176 °C. IR ν cm^{-1}: 3346 (NH_2), 1698 (CO). ^{1}H NMR δ ppm: 2.22 (6H, s, $2CH_3$), 4.71 (2H, s, CH_2CO), 6.92 (1H, s, $C_{5'}$–H), 7.56 (2H, s, NH_2), 7.99 (2H, d, J = 8.1 Hz, $C_{2,6}$–H), 8.22 (2H, d, J = 7.8 Hz, $C_{3,5}$–H). ^{13}C NMR δ ppm: 23.85 (2C), 38.43, 116.72, 126.62 (2C), 129.56 (2C), 139.74, 148.40, 167.65 (2C), 169.39, 194.83. HRMS calcd. for $C_{14}H_{15}N_3O_3S_2$ ($[M + H]^+$): 338.0628, found: 338.0622.

*4.1.1.13. 2-Chloro-5-{[(5-ethyl-2-pyrimidinyl)sulfanyl]acetyl}benzenesulfonamide (**1g**).* Yield 72%, mp 151–153 °C. IR ν cm^{-1}: 3300 (NH_2), 1705 (CO). ^{1}H NMR δ ppm: 1.16 (3H, t, J = 7.5 Hz, CH_3), 2.54 (2H, q, J = 7.5 Hz, CH_2), 4.81 (2H, s, CH_2CO), 7.83 (2H, s, NH_2), 7.88 (1H, d, J = 8.4 Hz, C_3–H), 8.31 (1H, dd, J = 2.1 Hz, J = 8.1 Hz, C_4–H), 8.48 (2H, s, $C_{4',6'}$–H), 8.56 (1H, d, J = 1.8 Hz, C_6–H). ^{13}C NMR δ ppm: 15.59, 22.86, 38.78, 128.98, 132.96, 133.62, 135.50, 136.03, 142.26 (2C), 157.81 (2C), 167.54, 193.19. HRMS calcd. for $C_{14}H_{14}ClN_3O_3S_2$ ($[M + H]^+$): 372.0238, found: 372.0243.

*4.1.1.14. 4-{[(5-Ethyl-2-pyrimidinyl)sulfanyl]acetyl}benzenesulfonamide (**2g**).* Yield 79%, mp 180–182 °C. IR ν cm^{-1}: 3245 (NH_2), 1706 (CO). ^{1}H NMR δ ppm: 1.16 (3H, t, J = 7.5 Hz, CH_3), 2.54 (2H, q, J = 7.5 Hz, CH_2), 4.83 (2H, s, CH_2CO), 7.58 (2H, s, NH_2), 8.00 (2H, d, J = 8.7 Hz, $C_{2,6}$–H), 8.22 (2H, d, J = 8.7 Hz, $C_{3,5}$–H), 8.48 (2H, s, $C_{4',6'}$–H). ^{13}C NMR δ ppm: 15.58, 22.86, 39.10, 126.73 (2C), 129.68 (2C), 132.97, 139.17, 148.57, 157.78 (2C), 167.68, 194.12. HRMS calcd. for $C_{14}H_{15}N_3O_3S_2$ ($[M + H]^+$): 338.0628, found: 338.0624.

*4.1.1.15. 2-Chloro-5-{[(5-propyl-2-pyrimidinyl)sulfanyl]acetyl}benzenesulfonamide (**1h**).* Yield 79%, mp 173–175 °C. IR ν cm^{-1}: 3348 (NH_2), 1704 (CO). ^{1}H NMR δ ppm: 0.87 (3H, t, J = 7.5 Hz, CH_3), 1.56 (2H, sextet, J = 7.5 Hz, CH_2), 2.48 (2H, t, J = 7.5 Hz, CH_2), 4.81 (2H, s, CH_2CO), 7.85 (2H, s, NH_2), 7.88 (1H, d, J = 8.1 Hz, C_3–H), 8.31 (1H, dd, J = 2.1 Hz, J = 8.4 Hz, C_4–H), 8.47 (2H, s, $C_{4',6'}$–H), 8.55 (1H, d, J = 2.1 Hz, C_6–H). ^{13}C NMR δ ppm: 14.08, 24.10, 31.46, 38.81, 128.97, 131.42, 132.97, 133.65, 135.48, 136.05, 142.25, 158.17(2C), 167.63, 193.19. HRMS calcd. for $C_{15}H_{16}ClN_3O_3S_2$ ($[M + H]^+$): 386.0394, found: 386.0392.

*4.1.1.16. 4-{[(5-Propyl-2-pyrimidinyl)sulfanyl]acetyl}benzenesulfonamide (**2h**).* Yield 75%, mp 165–167 °C. IR ν cm^{-1}: 3260 (NH_2), 1706 (CO). ^{1}H NMR δ ppm: 0.88 (3H, t, J = 7.2 Hz, CH_3), 1.56 (2H, sextet, J = 7.5 Hz, CH_2), 2.49 (2H, t, J = 7.8 Hz, CH_2), 4.83 (2H, s, CH_2CO), 7.59 (2H, s, NH_2), 8.00 (2H, d, J = 8.4 Hz, $C_{2,6}$–H), 8.24 (2H, d, J = 8.1 Hz, $C_{3,5}$–H), 8.47 (2H, s, $C_{4',6'}$–H). ^{13}C NMR δ ppm: 14.06, 24.06, 31.46, 39.13, 126.73 (2C), 129.67 (2C), 131.38, 139.15, 148.56, 158.12 (2C), 167.74, 194.10. HRMS calcd. for $C_{15}H_{17}N_3O_3S_2$ ($[M + H]^+$): 352.0784, found: 352.0781.

*4.1.1.17. 5-{[(5-Butylpyrimidin-2-yl)thio]acetyl}-2-chlorobenzenesulfonamide (**1i**).* Yield 84%, mp 124–126 °C. IR ν cm^{-1}: 3322 (NH_2), 1702 (CO). ^{1}H NMR δ ppm: 0.88 (3H, t, J = 7.5 Hz, CH_3), 1.28 (2H, sextet, J = 7.5 Hz, CH_2), 1.52 (2H, quintet, J = 7.5 Hz, CH_2), 2.48–2.53 (2H, m, CH_2), 4.82 (2H, s, CH_2CO), 7.85 (2H, s, NH_2), 7.88 (1H, d, J = 8.7 Hz, C_3–H), 8.32 (1H, dd, J = 1.8 Hz, J = 8.1 Hz, C_4–H), 8.47 (2H, s, $C_{4',6'}$–H), 8.56 (1H, d, J = 1.5 Hz, C_6–H). ^{13}C NMR δ ppm: 14.33, 22.28, 29.16, 32.98, 38.81, 128.99, 131.64, 132.97, 133.65, 135.48, 136.05, 142.26, 158.13 (2C), 167.58, 193.20. HRMS calcd. for $C_{16}H_{18}ClN_3O_3S_2$ ($[M + H]^+$): 400.0551, found: 400.0550.

*4.1.1.18. 4-{[(5-Butyl-2-pyrimidinyl)sulfanyl]acetyl}benzenesulfonamide (**2i**).* Yield 70%, mp 147–149 °C. IR ν cm^{-1}: 3275 (NH_2), 1706 (CO). ^{1}H NMR δ ppm: 0.89 (3H, t, J = 7.2 Hz, CH_3), 1.28 (2H, sextet, J = 7.2 Hz, CH_2), 1.52 (2H, quintet, J = 7.5 Hz, CH_2), 2.48–2.55 (2H, m, CH_2), 4.83 (2H, s, CH_2CO), 7.59 (2H, s, NH_2), 8.00 (2H, d, J = 8.4 Hz, $C_{2,6}$–H), 8.23 (2H, d, J = 8.4 Hz, $C_{3,5}$–H), 8.47 (2H, s, $C_{4',6'}$–H). ^{13}C NMR δ ppm: 14.31, 22.26, 29.14, 32.95, 39.12, 126.74 (2C), 129.68 (2C), 131.60, 139.16, 148.57, 158.09 (2C), 167.69, 194.12. HRMS calcd. for $C_{16}H_{19}N_3O_3S_2$ ($[M + H]^+$): 366.0941, found: 366.0940.

*4.1.1.19. 2-Chloro-5-[(2-pyrimidinylsulfanyl)acetyl]benzenesulfonamide (**1j**).* Yield 90%, mp 195–197 °C. IR ν cm^{-1}: 3325 (NH_2), 1708 (CO). ^{1}H NMR δ ppm: 4.85 (2H, s, CH_2CO), 7.23 (1H, t, J = 4.8 Hz, $C_{5'}$–H), 7.86 (2H, s, NH_2), 7.89 (1H, d, J = 8.1 Hz, C_3–H), 8.33 (1H, dd, J = 2.1 Hz, J = 8.1 Hz, C_4–H), 8.56 (1H, d, J = 2.1 Hz, C_6–H), 8.60 (2H, d, J = 4.8 Hz, $C_{4',6'}$–H). ^{13}C NMR δ ppm: 38.87, 118.15, 128.97, 133.00, 133.66, 135.43, 136.08, 142.26, 158.50 (2C), 170.49, 193.05. HRMS calcd. for $C_{12}H_{10}ClN_3O_3S_2$ ($[M + H]^+$): 343.9925, found: 343.9926.

*4.1.1.20. 4-[(2-Pyrimidinylsulfanyl)acetyl]benzenesulfonamide (**2j**).* Yield 79%, mp 186–188 °C. IR ν cm^{-1}: 3313, 3290 (NH_2), 1693 (CO). ^{1}H NMR δ ppm: 4.87 (2H, s, CH_2CO), 7.22 (1H, t, J = 4.8 Hz, $C_{5'}$–H), 7.62 (2H, s, NH_2), 8.01 (2H, d, J = 8.4 Hz, $C_{2,6}$–H), 8.25 (2H, d, J = 8.4 Hz, $C_{3,5}$–H), 8.59 (2H, d, J = 4.8 Hz, $C_{4',6'}$–H). ^{13}C NMR δ ppm: 39.22, 118.12, 126.75 (2C), 129.73 (2C), 139.06, 148.57, 158.48 (2C), 170.61, 193.93. HRMS calcd. for $C_{12}H_{11}N_3O_3S_2$ ($[M + H]^+$): 310.0315, found: 310.0313.

*4.1.1.21. 2-Chloro-5-[(phenylsulfanyl)acetyl]benzenesulfonamide (**1k**).* Yield 78%, mp 122–124 °C. IR ν cm^{-1}: 3363, 3257 (NH_2), 1689 (CO). ^{1}H NMR δ ppm: 4.70 (2H, s, CH_2CO), 7.20–7.24 (1H, m, $C_{4'}$–H), 7.29–7.35 (4H, m, $C_{2',3',5',6'}$–H), 7.82–7.86 (3H, m, NH_2, C_3–H), 8.27 (1H, d, J = 8.1 Hz, C_4–H), 8.48 (1H, s, C_6–H). ^{13}C NMR δ ppm: (38.87–41.05 – superposed with DMSO), 127.03, 129.12, 129.37(2C), 129.76(2C), 132.82, 134.04, 134.67, 135.40, 136.10, 142.27, 193.34. HRMS calcd. for $C_{14}H_{12}ClNO_3S_2$ ($[M + H]^+$): 342.0020, found: 342.0023.

*4.1.1.22. 4-[(Phenylsulfanyl)acetyl]benzenesulfonamide (**2k**).* Yield 75%, mp 145–147 °C. IR ν cm^{-1}: 3382, 3282 (NH_2), 1681 (CO). ^{1}H NMR δ ppm: 4.71 (2H, s, CH_2CO), 7.23–7.30 (1H, m, $C_{4'}$–H), 7.33–7.41 (4H, m, $C_{2',3',5',6'}$–H), 7.58 (2H, s, NH_2), 7.98 (2H, d, J = 8.4 Hz, $C_{2,6}$–H), 8.20 (2H, d, J = 8.4 Hz, $C_{3,5}$–H). ^{13}C NMR δ ppm: (39.45–41.11 – superposed with DMSO), 126.65 (2C), 126.98, 129.39 (2C), 129.75 (2C), 129.97 (2C), 135.58, 138.36, 148.62, 194.40. HRMS calcd. for $C_{14}H_{13}NO_3S_2$ ($[M + H]^+$): 308.0410, found: 308.0404.

4.1.2. Open and cyclic forms of the pyrimidinones

An investigation of the **1a**–**j** and **2a**–**j** compound structures by NMR spectrocopy showed that the ^{1}H and ^{13}C NMR spectra of pyrimidinones **1a**–**e**, **2a**–**e** in DMSO-d_6 solution contained two sets of signals. These results led to a suggestion that this phenomenon could be due to the existence of compounds **1a**–**e** and **2a**–**e** in two forms: open chain **I** and cyclic **II** (Scheme 3).

Especially large differences were observed for signals of SCH_2 group protons in the ^{1}H NMR spectra (Table 2). This signal of open chain form **I** was observed as a singlet in the 4.72–4.94 ppm region, while SCH_2 protons of cyclic form **II** appeared as doublets with J = 12–13 Hz at 3.56–3.73 ppm. The geminal-type spin–spin coupling of SCH_2 protons arises from their non-equivalency in the cyclic form **II**. ^{13}C NMR spectra of compounds **1a**–**e** and **2a**–**e** gave additional evidence for the existence of equilibria between open chain and cyclic forms of compounds **1a**–**e** and **2a**–**e** in a solution. The main differences in the ^{13}C NMR spectra, as expected, were observed for carbon atoms taking part in the transformation (Table 2). Thus, the signal for carbon of the SCH_2 group in open chain form **I** was observed at 37.34–39.27 ppm. In the ^{13}C NMR

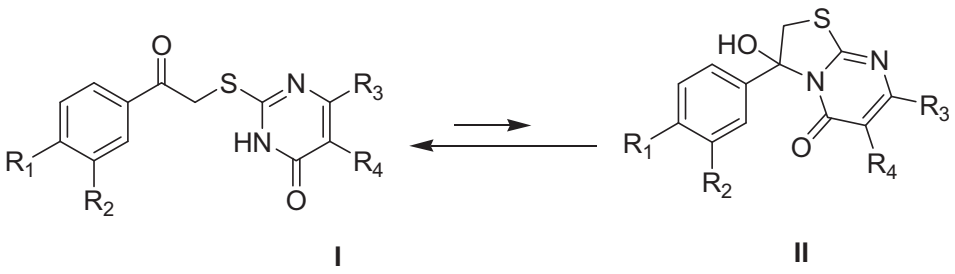

1a: R_1=Cl, R_2=SO_2NH_2, R_3=Me, R_4=H,
2a: R_1=SO_2NH_2, R_2=H, R_3=Me, R_4=H,
1b: R_1=Cl, R_2=SO_2NH_2, R_3=Me, R_4=Bn,
2b: R_1=SO_2NH_2, R_2=H, R_3=Me, R_4=Bn,
1c: R_1=Cl, R_2=SO_2NH_2, R_3=Pr, R_4=H,
2c: R_1=SO_2NH_2, R_2=H, R_3=Pr, R_4=H,
1d: R_1=Cl, R_2=SO_2NH_2, R_3=t-Bu, R_4=H,
2d: R_1=SO_2NH_2, R_2=H, R_3=t-Bu, R_4=H,
1e: R_1=Cl, R_2=SO_2NH_2, R_3=H, R_4=CO_2Et,
2e: R_1=SO_2NH_2, R_2=H, R_3=H, R_4=CO_2Et,

Scheme 3. Open chain and cyclic forms of compounds **1a**–**e** and **2a**–**e**.

spectra of cyclic form **II**, a signal for this carbon was slightly shifted to a region of lower fields and was observed in the 42.36–43.03 ppm region. Moreover, the open chain forms of compounds **1a**–**e** and **2a**–**e** were well characterized by the C=O group carbon signal ranging from 192.25 to 194.11 ppm. The C–OH group carbon signal of cyclic form **II** was observed in the 95.90–97.81 ppm range. Thus, the obtained NMR spectral data showed the presence of two forms of compounds (**1a**–**e** and **2a**–**e**) in DMSO-d_6 solution. The ratio **I**:**II** was 1.0:0.3, as calculated from integral intensities of SCH_2 signals of ^{1}H NMR spectra. A similar ratio of 1.0:0.3 was previously observed for similar compounds, 2-(carbonylmethylthio)-4-pyrimidinones [20].

4.2. Protein preparation

Expression and purification of CA I, CA II, CA VII, and CA XIII was previously described: CA I in, [21], CA II in [22] and CA VII and XIII in [11].

4.3. Determination of compound binding to CAs

4.3.1. Thermal shift assay

Thermal shift assay experiments were performed in a Corbett Rotor-Gene 6000 (QIAGEN Rotor-Gene Q) instrument using the blue channel (excitation 365 ± 20, detection 460 ± 15 nm). Samples contained 10 μM protein, 0–200 μM ligand, 50 μM solvatochromic dye ANS (8-anilino-1-naphthalene sulfonate), and 50 mM phosphate buffer containing 100 mM NaCl at pH 7.0, with the final DMSO concentration at 2%. The applied heating rate was 1 °C/min. Data analysis was performed as previously described [21,23]

4.3.2. Isothermal titration calorimetry

ITC experiments were performed using ITC_{200} or VP-ITC instruments (Microcal, Inc., Northampton, USA) with 5–20 μM protein solution in the cell and 50–200 μM of the ligand solution in the syringe. A typical experiment consisted of 18 or 25 injections (2 or 10 μl each) within 2 or 3 min intervals. Variation of the time period between injections enabled the detection and elimination of possible kinetic effects that may distort the binding data. Experiments were carried out at 37 °C in a 50 mM phosphate buffer containing 100 mM NaCl at pH 7.0, with a final DMSO concentration of 2%.

4.4. Crystallography

4.4.1. Crystallization

Crystallization of CA II that was concentrated to 40–60 mg/ml was started by mixing equal volumes of protein solution with reservoir buffer in sitting drops. Crystallization solutions were prepared by mixing 1 M Na-Bicine, pH 9 to final concentration 0.1 M with 2.7 M Na-Malonate, pH 7, so that the final concentration of malonate ranged from 1.2 to 2.1 M. Crystals belonging to the $P2_1$

Table 2
Characteristic chemical shifts of ^{1}H and ^{13}C NMR spectra of open chain **I** and cyclic **II** forms of compounds **1a**–**e** and **2a**–**e** in DMSO-d_6 solution.

Compound	^{13}C NMR spectra				^{1}H NMR spectra	
	$S\underline{C}H_2C$=O in I	$S\underline{C}H_2OH$ in II	$SCH_2\underline{C}$=O in I	$SCH_2\underline{C}OH$ in II	SCH_2CO in I	SCH_2 in II
1a	37.94	42.37	193.24	96.08	4.74 (2H, s)	3.58 (0.32H, d, J = 12.9 Hz), 3.66 (0.32H, d, J = 12.3 Hz)
2a	38.30	42.36	194.11	96.70	4.76 (2H, s)	3.56 (0.31H, d, J = 12.3 Hz), 3.63 (0.31H, d, J = 12.3 Hz)
1b	37.73	42.56	193.22	96.37	4.73 (2H, s)	3.57–3.70 (3.24H, m, $\underline{CH_2}COH$, CH_2Ph, o, c)
2b	38.14	42.60	194.07	96.97	4.76 (2H, s)	3.59 (0.32H, d, J = 12.0 Hz), 3.65 (0.32H, d, J = 12.0 Hz)
1c	37.75	42.38	193.15	96.05	4.72 (2H, s)	3.59 (0.31H, d, J = 12.6 Hz), 3.66 (0.31H, d, J = 12.6 Hz)
2c	38.14	42.41	193.90	96.61	4.75 (2H, s)	3.57 (0.32H, d, J = 12.6 Hz), 3.64 (0.32H, d, J = 12.3 Hz)
1d	37.35	42.37	192.25	95.90	4.82 (2H, s)	3.57 (0.31H, d, J = 12.6 Hz), 3.68 (0.31H, d, J = 12.3 Hz)
2d	37.34	42.39	192.98	96.45	4.83 (2H, s)	3.59 (0.25H, d, J = 12.9 Hz), 3.66 (0.25H, d, J = 12.0 Hz)
1e	38.93	42.97	192.16	97.20	4.92 (2H, s)	3.64 (0.28H, d, J = 12.9 Hz), 3.76 (0.28H, d, J = 12.6 Hz)
2e	39.27	43.03	193.03	97.81	4.94 (2H, s)	3.65 (0.28H, d, J = 12.6 Hz), 3.73 (0.28H, d, J = 12.6 Hz)

Table 3
X-ray crystallographic data collection and refinement statistics. All datasets are collected at 100 K. All crystals belong to $P2_1$ space group.

Ligand	**1f**	**1g**	**2a**	**2i**	**2f**	**2j**
PDB ID	3S9T	3SAX	3S8X	3SAP	3SBH	3SBI
Parameters of the unit cell, Å $\alpha = \gamma = 90°$	$a = 42.01$, $b = 41.06$, $c = 71.84$, $\beta = 104.15°$	$a = 42.22$, $b = 41.17$, $c = 72.20$, $\beta = 104.20°$	$a = 42.21$, $b = 41.18$, $c = 71.92$, $\beta = 104.29°$	$a = 42.02$, $b = 40.96$, $c = 71.74$, $\beta = 104.08°$	$a = 42.09$, $b = 41.09$, $c = 71.84$, $\beta = 104.17°$	$a = 42.35$, $b = 41.31$, $c = 72.24$, $\beta = 104.25°$
Resolution, Å	1.30	1.10	1.30	1.75	1.65	1.40
Reflections unique (total)	58,642 (409,726)	92,709 (668,605)	56,499 (431,988)	23,825 (171,710)	28,165 (213,598)	46,467 (277,941)
Completeness (%) Overall (outer shell)	100.0 (100.0)	93.4 (79.2)	95.9 (93.6)	99.0 (98.6)	97.7 (96.8)	97.1 (95.7)
I/σ_I Overall (outer shell)	14.0 (2.7)	15.5 (4.8)	26.2 (3.5)	30.3 (7.9)	30.7 (9.7)	25.2 (4.6)
R_{merge} overall (outer shell)	0.129 (0.368)	0.068 (0.275)	0.064 (0.380)	0.058 (0.266)	0.058 (0.278)	0.043 (0.344)
Number of atoms (if alt. conformations are present, then only one is included)	2406	2458	2339	2292	2418	2419
Number of solvent molecules	309	377	248	195	303	320
Number of bound buffer molecule atoms	19	19	19	23	27	19
R_{cryst} (R_{free}) Test set size 10%	0.143 (0.192)	0.126 (0.158)	0.142 (0.179)	0.182 (0.229)	0.172 (0.228)	0.133 (0.183)
RMS bonds/angles	0.034 (2.64)	0.029 (2.52)	0.028 (2.35)	0.015 (1.49)	0.029 (2.34)	0.029 (2.23)
Average B-factors (Å^2)	14.2	12.4	16.2	17.6	15.5	14.6
Main chain	11.3	9.6	13.5	15.6	12.6	11.7
Side chains	14.3	12.0	16.5	17.5	15.1	14.2
Solvent	24.7	23.7	25.6	24.7	24.8	25.2
Ions	7.2	5.4	8.1	10.2	8.0	6.2
Inhibitor	14.3	15.0	16.8	34.4	24.5	12.2
Cofactors	23.6	20.9	27.9	37.5	33.1	29.2

$R_{merge} = \sum_h \sum_{i=1}^{n_h} |\langle I_h \rangle - I_{hi}| / \sum_h \sum_{i=1}^{n_h} |I_{hi}|$, where I_{hi} is an intensity value of the i-th measurement of reflection h, $h = (h, k, l)$, sum Σ_h runs overall measured reflections, and $\langle I_h \rangle$ is an average measured intensity of the reflection $\boldsymbol{h}$. The n_h is the number of measurements of reflection h.

space group grew within several days. Crystals were soaked with a 0.5 mM solution of the ligand prepared by mixing of 50 mM solution of the ligand in DMSO with 50 μl of reservoir buffer from the crystallization plate.

4.4.2. Data collection and structure determination

Diffraction data from all complexes of CA II with compounds selected for crystallographic studies were collected at the EMBL X11, X12 and X13 beamlines at the DORIS storage ring (DESY, Hamburg). Datasets were processed using MOSFLM [24,25] and SCALA [26]. Initial phases for molecular replacement were calculated with 3HLJ PDB entry [21] omitting heteroatoms and ligands. REFMAC [27] and COOT [28] were used for structure refinement and model building. Inhibitors were modeled with the help of DSVisualizer 1.7 [29] (Accelrys), and corresponding topology and parameters for refinement were generated using LIBREFMAC [30]. The statistics of data collection and refinement are presented in Table 3. Coordinates and structure factors are deposited in the RCSB Protein Databank, and PDB IDs are given in Table 3.

4.5. Computational docking details

The scaffolds for building the compounds were obtained from the PDB entries 3M96 [10] (series of chlorinated compounds) and **2j** (compounds without chlorine). The construction and minimization of the non-scaffold part of the molecule was performed using the Avogadro program [31], keeping the scaffold frozen. Oxo-tautomer was used for the hydroxy-pyrimidine series.

Docking was performed with the Vdock program using the default settings [12]. CHARMM22 force field [32] was used for the proteins, and the modified Dreiding force field [33] and VeraChem's partial atomic charges [34] were applied for the small molecules. The solvent effect was modeled with the distance-dependent dielectric approach, $\varepsilon_{ij} = 4r_{ij}$. Poisson–Boltzmann surface area (PBSA) approach was used to evaluate the binding affinities of ligands to CA II (Gibbs free energy of binding), employing the following equation:

$$\Delta G_{bind} \approx \Delta\alpha\left(V^{el} + V^{PB}\right) + \beta\Delta V^{vdw} + \gamma\Delta SASA + \delta$$

where V^{el} - electrostatic interaction energy, V^{PB} - Poisson–Boltzmann electrostatic energy correction due to solvation, V^{vdw} - van der Waals interaction energy, SASA - solvent accessible surface area, and α, β, γ, δ are fitted parameters.

To compute Poisson–Boltzmann (PB) and Solvent Accessible Surface Area for the PBSA calculations, the APBS v. 1.2.1 [35] and SIMS [36] programs were used. For the PB calculation, protein and solvent dielectric constants were 2 and 78, respectively. For the SASA calculation, solvent probe radius was 1.4 Å and smoothing radius was 0.4 Å.

5. Associated content

PDB accession codes for the crystal structures of CA II with compounds **1f**, **1g**, **2a**, **2i**, **2f**, and **2j** are 3SAX, 3S8X, 3SAP, 3SBH, and 3SBI, respectively.

Acknowledgments

This research was funded by a grant (No. LIG-16/2010) from the Research Council of Lithuania. Diffraction data were collected at the EMBL/DESY, Hamburg, X11, X12, X13 beamlines. Access to the measurement facilities was funded from the European Community's Seventh Framework Programme (FP7/2007-2013) under grant agreement no. 26716. EM travel to DESY, Hamburg was supported from the Research Council of Lithuania (project No. C-01/2008, registration No. C-08027), SG and GT travel was supported by the FP7-REGPOT-2009-1 program (project 245721 MoBiLi). The authors thank Zita Liutkevičiūtė for help with the mass spectrometry analysis of the synthetic compounds and local contacts at the EMBL beamlines for their help with beamline operation.

Appendix. Supplementary data

Supplementary data associated with this article can be found, in the online version, at doi:10.1016/j.ejmech.2012.02.050.

References

[1] R.L. Mikulski, D.N. Silverman, Proton transfer in catalysis and the role of proton shuttles in carbonic anhydrase, Biochim. Biophys. Acta 1804 (2010) 422–426.
[2] C.T. Supuran, Carbonic anhydrases: novel therapeutic applications for inhibitors and activators, Nat. Rev. Drug Discov. 7 (2008) 168–181.
[3] S. Pastorekova, S. Parkkila, J. Pastorek, C.T. Supuran, Carbonic anhydrases: current state of the art, therapeutic applications and future prospects, J. Enzym. Inhib. Med. Chem. 19 (2004) 199–229.
[4] W.S. Sly, P.Y. Hu, Human carbonic anhydrases and carbonic anhydrase deficiencies, Annu. Rev. Biochem. 64 (1995) 375–401.
[5] C.T. Supuran, A. Scozzafava, Carbonic anhydrases as targets for medicinal chemistry, Bioorg. Med. Chem. 15 (2007) 4336–4350.
[6] A. Scozzafava, A. Mastrolorenzo, C.T. Supuran, Carbonic anhydrase inhibitors and activators and their use in therapy, Expert Opin. Ther. Patents 16 (2006) 1627–1664.
[7] C.T. Supuran, A. Scozzafava, A. Casini, Carbonic anhydrase inhibitors, Med. Res. Rev. 23 (2003) 146–189.
[8] C.T. Supuran, A. Scozzafava, J. Conway, Carbonic Anhydrase – Its Inhibitors and Activators, CRC Press, Boca Raton, FL, USA, 2004.
[9] S. Pastorekova, J. Kopacek, J. Pastorek, Carbonic anhydrase inhibitors and the management of cancer, Curr. Top. Med. Chem. 7 (2007) 865–878.
[10] E. Capkauskaite, L. Baranauskiene, D. Golovenko, E. Manakova, S. Grazulis, S. Tumkevicius, D. Matulis, Indapamide-like benzenesulfonamides as inhibitors of carbonic anhydrases i, ii, vii, and xiii, Bioorg. Med. Chem. 18 (2010) 7357–7364.
[11] J. Sudzius, L. Baranauskiene, D. Golovenko, J. Matuliene, V. Michailoviene, J. Torresan, J. Jachno, R. Sukackaite, E. Manakova, S. Grazulis, S. Tumkevicius, D. Matulis, 4-[*n*-(Substituted 4-pyrimidinyl)amino]benzenesulfonamides as inhibitors of carbonic anhydrase isozymes i, ii, vii, and xiii, Bioorg. Med. Chem. 18 (2010) 7413–7421.
[12] V. Kairys, M.K. Gilson, Enhanced docking with the mining minima optimizer: acceleration and side-chain flexibility, J. Comput. Chem. 23 (2002) 1656–1670.
[13] P.A. Kollman, I. Massova, C. Reyes, B. Kuhn, S. Huo, L. Chong, M. Lee, T. Lee, Y. Duan, W. Wang, O. Donini, P. Cieplak, J. Srinivasan, D.A. Case, T.E. Cheatham, Calculating structures and free energies of complex molecules: combining molecular mechanics and continuum models, Acc. Chem. Res. 33 (2000) 889–897.
[14] A.D. Scott, C. Phillips, A. Alex, M. Flocco, A. Bent, A. Randall, R. O'Brien, L. Damian, L.H. Jones, Thermodynamic optimisation in drug discovery: a case study using carbonic anhydrase inhibitors, Chem. Med. Chem. 4 (2009) 1985–1989.
[15] H. Oelschlager, 3-Alkyl-6-halogen-aniline aus p-halogenierten fettaromatischen ketonen, Justus Liebigs Ann. Chem. 641 (1961) 81–94.
[16] T. Fujikura, K. Miigata, S. Hashimoto, K. Imai, T. Takenaka, Studies on benzenesulfonamide derivatives with alpha- and beta-adrenergic antagonistic and antihypertensive activities, Chem. Pharm. Bull. (Tokyo) 30 (1982) 4092–4101.
[17] B.R. Baker, R.E. Schaub, J.P. Joseph, F.J. McEvoy, J.H. Williams, An antimalarial alkaloid from hydrangea. xviii. derivatives of 4-pyrimidone, J. Org. Chem. 18 (1953) 133–137.
[18] G.W. Anderson, I.F. Halverstadt, W.H. Miller, R.O. Roblin, 5- and 6-Substituted 2-thiouracils, J. Am. Chem. Soc. 67 (1945) 2197–2200.
[19] V.R. Kruse, E. Breitmaier, 2,5-Bisubstituierte pyrimidine aus 2-alkyl-3-athoxyacroeinen, Chemiker-Zeitung 101 (1977) 305–306.
[20] H.F. Andrew, C.K. Bradsher, A new synthesis of thiazolo[3.2-*a*]pyrimidinones, J. Heterocycl. Chem. 4 (1967) 577–581.
[21] L. Baranauskiene, M. Hilvo, J. Matuliene, D. Golovenko, E. Manakova, V. Dudutiene, V. Michailoviene, J. Torresan, J. Jachno, S. Parkkila, A. Maresca, C.T. Supuran, S. Grazulis, D. Matulis, Inhibition and binding studies of carbonic anhydrase isozymes i, ii and ix with benzimidazo[1,2-*c*][1,2,3]thiadiazole-7-sulphonamides, J. Enzym. Inhib. Med. Chem. 25 (2010) 863–870.
[22] P. Cimmperman, L. Baranauskiene, S. Jachimoviciute, J. Jachno, J. Torresan, V. Michailoviene, J. Matuliene, J. Sereikaite, V. Bumelis, D. Matulis, A quantitative model of thermal stabilization and destabilization of proteins by ligands, Biophys. J. 95 (2008) 3222–3231.
[23] D. Matulis, J.K. Kranz, F.R. Salemme, M.J. Todd, Thermodynamic stability of carbonic anhydrase: measurements of binding affinity and stoichiometry using thermofluor, Biochemistry 44 (2005) 5258–5266.
[24] A. G. W. Leslie, Recent changes to the mosflm package for processing film and image plate data, Joint CCP4 + ESF-EAMCB Newsletter on Protein Crystallography 26.
[25] A.G.W. Leslie, The integration of macromolecular diffraction data, Acta Crystallogr. D Biol. Crystallogr. 62 (2006) 48–57.
[26] P. Evans, Scaling and assessment of data quality, Acta Crystallogr. D Biol. Crystallogr. 62 (2006) 72–82.
[27] G.N. Murshudov, A.A. Vagin, E.J. Dodson, Refinement of macromolecular structures by the maximum-likelihood method, Acta Crystallogr. D Biol. Crystallogr. 53 (1997) 240–255.
[28] P. Emsley, K. Cowtan, Coot: model-building tools for molecular graphics, Acta Crystallogr. D Biol. Crystallogr. 60 (2004) 2126–2132.
[29] Discovery Studio Visualizer 2.0 Free Life Science Visualizer (2009).
[30] N. Collaborative Computational Project, The ccp4 suite: programs for protein crystallography, Acta Cryst. D 50 (1994) 760–763.
[31] Avogadro, Avogadro: An Open-Source Molecular Builder and Visualization Tool. Version 1.0.0 (2009).http://avogadro.openmolecules.net/.
[32] A.D. MacKerell, D. Bashford, M. Bellott, R.L. Dunbrack, J.D. Evanseck, M.J. Field, S. Fischer, J. Gao, H. Guo, S. Ha, D.J. McCarthy, L. Kuchnir, K. Kuczera, F.T.K. Lau, C. Mattos, S. Michnick, T. Ngo, D.T. Nguyen, B. Prodhom, W.E. Reiher, B. Roux, M. Schlenkrich, J.C. Smith, R. Stote, J. Straub, M. Watanabe, J. Wiorkiewicz-Kuczera, D. Yin, M. Karplus, All-atom empirical potential for molecular modeling and dynamics studies of proteins, J. Phys. Chem. B 102 (1998) 3586–3616.
[33] S.L. Mayo, B.D. Olafson, W.A. Goddard, Dreiding: a generic force field for molecular simulations, J. Phys. Chem. 94 (1990) 8897–8909.
[34] M.K. Gilson, H.S.R. Gilson, M.J. Potter, Fast assignment of accurate partial atomic charges: an electronegativity equalization method that accounts for alternate resonance forms, J. Chem. Inf. Comput. Sci. 43 (2003) 1982–1997.
[35] N.A. Baker, D. Sept, S. Joseph, M.J. Holst, J.A. McCammon, Electrostatics of nanosystems: application to microtubules and the ribosome, Proc. Natl. Acad. Sci. U.S.A. 98 (2001) 10037–10041.
[36] Y. Vorobjev, J. Hermans, Sims: computation of a smooth invariant molecular surface, Biophysical J. 73 (1997) 722–732.
[37] P.J. Kraulis, Molscript: a program to produce both detailed and schematic plots of protein structures, J. Appl. Cryst. 24 (1991) 946–950.
[38] E.A. Merritt, D.J. Bacon, Raster3d: photorealistic molecular graphics, Methods Enzymol. 277 (1997) 505–524.
[39] R.M. Esnouf, Further additions to molscript version 1.4, including reading and contouring of electron-density maps, Acta Crystallogr. D Biol. Crystallogr. 55 (1999) 938–940.